Phosphorylation of Merlin by Aurora A kinase appears necessary for mitotic progression

Vinay Mandati, Laurence Del Maestro, Florent Dingli, Berangère Lombard, Damarys Loew, Nicolas Molinie, Stephane Romero, Daniel Bouvard, Daniel Louvard, Alexis Gautreau, et al.

JBC Papers in Press. Published on July 11, 2019 as Manuscript RA118.006937
The latest version is at http://www.jbc.org/cgi/doi/10.1074/jbc.RA118.006937

Phosphorylation of Merlin by Aurora A kinase appears necessary for mitotic progression

Vinay Mandati[1,2], Laurence Del Maestro[1,3], Florent Dingli[4], Bérangère Lombard[4], Damarys Loew[4], Nicolas Molinie[5], Stephane Romero[5], Daniel Bouvard[7], Daniel Louvard[1], Alexis M. Gautreau[5], Eric Pasmant[6] and Dominique Lallemand[1,6]

The first two authors contributed equally to this work.

1- CNRS, UMR144, Institute Curie, PSL Research University, Paris, France.
2- Present address: Cold Spring Harbor Laboratory, Cold Spring Harbor, New-York 11724, USA.
3- Present address: CNRS, Université de Paris, Epigenetics and Cell Fate, UMR 7216 CNRS, Paris, France.
4- Laboratoire de Spectrométrie de Masse Protéomique, Institute Curie, PSL Research University, Paris, France.
5- BIOC, CNRS UMR7654, Institut Polytechnique de Paris, F-91128 Palaiseau, France.
6- Present address: Insitut Cochin, INSERM U1016, Université Paris Descartes, Sorbonne Paris Cité, Paris, France.
7- INSERM, Institut Albert Bonniot U823, F-38042, Grenoble, France.

Running title: *Merlin regulates mitotic progression*

To whom correspondence should be addressed: Dominique Lallemand, Insitut Cochin, INSERM U1016, Université Paris Descartes, Sorbonne Paris Cité, Paris, France. Mail: dominique.lallemand@inserm.fr. Telephone: 33 1 70 64 94 02.

Keywords: Merlin/NF2, phosphorylation, Mitosis, Aurora A, Ezrin, Tubulin, tumor suppressor gene, Neurofibromatosis type 2, cell proliferation.

Abstract

Although Merlin function as a tumor suppressor and regulator of mitogenic signaling networks such as the Ras/rac, Akt or Hippo pathways is well documented,in mammals as well as in insects, its role during cell cycle progression remains unclear. In this study, using a combination of approaches, including FACS analysis, time-lapse imaging, immunofluorescence microscopy and co-immunoprecipitation, we show that Ser-518 of Merlin is a substrate of the Aurora A kinase during mitosis and that its phosphorylation facilitates the phosphorylation of a newly discovered site, Thr-581. We found that the expression in Hela cells of a Merlin variant that is phosphorylation-defective on both sites leads to a defect in centrosomes and mitotic spindles positioning during metaphase and delays the transition from metaphase to anaphase. We also show that the dual mitotic phosphorylation not only reduces Merlin binding to microtubules but also timely modulates Ezrin interaction with the cytoskeleton. Finally, we identify several point mutants of Merlin associated with Neurofibromatosis type 2 that display an aberant phosphorylation profile along with defective α-tubulin binding properties. Altogether, our findings of an Aurora A–mediated interaction of Merlin with α-tubulin and Ezrin suggest a potential role for Merlin in cell cycle progression.

Introduction

The loss of Merlin expression results in tumor development in humans, a condition known as Neurofibromatosis type 2 (1-3). Merlin, the product of the *NF2* tumor suppressor gene, inhibits cell proliferation by regulating signaling mediated by Rac1 and Ras GTPases or by mTorc1 and 2. At the plasma membrane, Merlin attenuates growth factor receptors expression and activity in both *Drosophila* and mammal (4-9). In addition, Merlin exerts its growth suppressive function in the nucleus where it inhibits the DCAF ubiquitin ligase activity (10). Finally, Merlin is a major regulator of the Hippo signaling pathway by inhibiting the nuclear accumulation of the co-transcription factor Yap and Taz in various organisms (11, 12). Although these mechanisms initially appeared distinct, cross talks were identified between several of them (13-15).

How Merlin modulates mitogenic signaling is extensively studied. In contrast, little information is available on a possible role in regulating cell cycle progression. In glioma and osteosarcoma cell lines, Merlin is nuclear early in G1 and gets exported toward the plasma membrane before S phase entry (16). Also, an interaction between Merlin and HEI10 was reported. HEI10 is involved in the regulation of cyclin B levels (17). However, no specific role of its interaction with Merlin was identified in the control of cell cycle progression. More recently *Hebert et al.,* demonstrated that Merlin regulates polarized cell division by restricting the cortical distribution of Ezrin necessary for centrosome positioning and proper orientation of cell division (18). Indeed, Ezrin, Radixin and Moesin (ERM) have been implicated in several aspects of mitotic progression. In *Drosophila* cells, Moesin activation by phosphorylation during mitosis increases the cortical rigidity necessary for proper spindle morphogenesis and chromosome alignment (19, 20). Moesin also regulates spindle length during metaphase and cell shape at a later stage of mitosis (21). In mammalian cells, the phosphorylation of the ERM by the kinase Slk during mitosis is key to the proper orientation of spindle (22). Interestingly, Merlin was shown to directly bind to microtubules and promote their stabilization (23, 24) but the functional consequences, were not investigated, notably during mitosis.

These observations suggest that Merlin plays a role in cell cycle progression and more specifically during mitosis. In the present study, we show that Merlin is a substrate for Aurora A kinase on the main regulatory serine 518, during mitosis. This event facilitates the phosphorylation of a second, newly discovered site at position 581 that is specific of Merlin isoform 1. When Merlin dual phosphorylation is compromised, it leads to a defect in the stabilization of mitotic spindle orientation prior to metaphase, delaying the onset of anaphase. At the mechanistic level, we show that phosphorylation on S518 controls Merlin interaction with α-tubulin whereas T581 phosphorylation modulates Merlin binding to Ezrin and subsequently Ezrin interactions with both actin and α-tubulin. Importantly, specific patient mutations affecting the FERM (Four point one Ezrin Radixin Moesin) domain of Merlin result in abnormal phosphorylation profile and α-tubulin binding properties, in some case associated with a delay in mitotic progression. Altogether our observations suggest that tight regulation of Merlin by Aurora A kinase is involved in mitotic progression via regulated binding to α–tubulin and Ezrin and is compromised by mutations found in Neurofibromatosis type 2 patients.

Results

Aurora A binds and phosphorylates Merlin in vitro and in vivo during mitosis

The Aurora A kinase phosphorylates a variety of substrates during the cell cycle progression. The phosphorylation sites contain a conserved arginine in -2 position relative to the target serine residue, and leucine is frequently found in -1 (25). A close examination of the sequence surrounding serine 518 of Merlin suggests a phosphorylation site for Aurora A, with arginine and a leucine in position 516 and 517 respectively (Figure 1A). To test if Merlin could be a substrate for Aurora A in vitro, GFP-Merlin was immunoprecipitated from interphasic HEK293 cells, dephosphorylated with alkaline phosphatase and then incubated with recombinant GST-Aurora A. The same procedure was performed with GFP-Merlin mutant S518A, as a negative control. Using a specific antibody to p-

S518, we could show that Aurora A efficiently phosphorylates this site in vitro (Figure 1B).

Endogenous phospho-Merlin could not reproducibly be detected in total extracts from Hela cells, likely due to a low affinity of the pS518 antibody and low levels of Merlin expression. Therefore, we generated Hela cells overexpressing Merlin isoform 1 under the tet-inducible promoter (Supplementary Figure 1A). Mitotic extracts were prepared from detached mitotic cells following overnight nocodazole block. The remaining attached cells were collected as interphasic population. As presented in Figure 1C, the phosphorylation of S518 was much higher (more than 5 times) in mitosis than during interphase.

Mitotic Hela cells overexpressing Merlin isoform I were then treated with the Aurora A specific inhibitor MLN8054. We observed a clear reduction of Merlin phosphorylation on S518 (Figure 1D). On the contrary, Aurora B inhibitor ZM4474 (Figure 1 E) had no effect. To confirm these results on endogenous Merlin, we treated mitotic HEK293 cells, expressing higher levels of Merlin than Hela cells, with MLN8054. We observed that S518 phosphorylation of immunoprecipitated Merlin dropped by 80% when compared to untreated cells (Figure 1F).

Finally, we could co-precipitate endogenous Aurora A kinase with GFP-Merlin from mitotic extracts. Interestingly, although the S518 phosphorylation site is close to the C-terminal end, the binding site of Aurora A lies within the FERM domain (Figure 1G). Aurora A did not co-immunoprecipitate with the patient-derived Merlin ∂2-3 mutant lacking amino acids 38 to 121 of the FERM domain (26) (Figure 1H) and the phosphorylation of S518 was drastically reduced in mitosis when compared to WT Merlin (Figure 1I). Altogether, our results demonstrate that Merlin is a bona fide substrate for Aurora A during mitosis.

A new site is phosphorylated during mitosis and is specific of Merlin isoform 1

A search for new phosphorylation sites of Merlin, by mass spectrometry, identified T581 in extracts from 293 HEK cells (Figure 2A). S518 and T581 were the two strongest peaks visible by a proteomic approach. Interestingly, T581 is specific of Merlin isoform 1 (Figure 2B). We raised a specific antibody against a peptide containing the phosphorylated T581. By western-blot, a weak signal was observed in asynchronous population but only when Merlin was overexpressed. The signal was abolished when T581 was changed for an alanine demonstrating the specificity of the antibody (Figure 2C). As was observed with S518, the phosphorylation of T581 was much more pronounced in mitosis than during interphase (Figure 2D). Importantly, T581 phosphorylation was detected in mouse kidney extracts in the context of a proteomic screen of mouse phosphoproteins. pS518 was detected more frequently than pT581 (https://phosphomouse.hms.harvard.edu/). This suggests that the phosphorylation of T581 might be limited compared to S518.

The sequence surrounding T581 doesn't closely match any known kinase consensus site. When we treated the mitotically arrested Hela cells with MLN8054, there was no decrease of T581 phosphorylation (Figure 2E) and Aurora A did not phosphorylate T581 in vitro indicating that this site is not a substrate for this kinase. We confirmed that T581 was not a substrate for Aurora B or C, or Slik. Also, Lats1/2 kinases, which were shown to interact with and be regulated by Aurora kinases (27) and that can bind the FERM domain of Merlin did not appear to phosphorylate Merlin during mitosis (Supplementary Figure 1B and 1C). Thus, it appears that T581 is the target of a kinase that is activated during mitosis and remains to be identified.

Phosphorylation of S518 by Aurora A in mitosis facilitates the phosphorylation of T581

It was previously shown that S518 phosphorylation facilitates the phosphorylation of S10, enabling Merlin degradation by the proteasome (28). We thus tested if phosphorylation of S518 and T581 could influence each other. To do so, we compared the phosphorylation of each site, during mitosis, when the second site is mutated to an alanine (A) or to aspartic acid (D). Mutations of T581 had no impact on the phosphorylation of S518. However, T581 was more efficiently phosphorylated, when

S518 was changed for an aspartic acid as opposed to an alanine (Figure 2F-G). Hence our data show that phosphorylation of S518 facilitates the phosphorylation of T581 during mitosis. It is possible that S518 phosphorylation creates a new binding site for the kinase that targets T581. In addition, it is also conceivable that S518 phosphorylation changes Merlin conformation facilitating the binding of a second kinase.

Impaired phosphorylation of Merlin during mitosis delays metaphase exit

Our results show that both S518 and T581 of Merlin are strongly phosphorylated during mitosis. We next investigated the consequences of the expression of double alanine (518A/581A- referred as AA hereafter) or aspartic acid substitutions (518D/581D- referred as DD hereafter) mutants in Hela cells during this phase of the cell cycle (Merlin mutants expression in Hela cells is shown in Supplementary Figure 1D). Using video microscopy (Figure 3A), their impact on mitotic progression was evaluated by measuring the interval between nuclear envelope breakdown (NEB) and the onset of anaphase (sister chromatid separation, SCS). A comparison has been made with uninduced Hela cells after we confirmed that wild-type Merlin overexpression had no effect on mitosis duration (Supplementary Figure 2). The expression of the dual aspartic acid mutant (DD), that mimics the doubly phosphorylated state of Merlin observed during mitosis, induced a very modest increase of the duration of NEB to SCS (Figure 3A lower panel, 3B right panel). The expression of the dual AA mutant, on the other hand, had a much more drastic effect, doubling the NEB to SCS transition time (Figure 3A upper panel, 3B left panel). More precisely, we could show that the longer mitosis is due to an increased duration of pro-metaphase to anaphase transition. Anaphase starts when the two centrosomes stabilize on the same plane at cellular poles providing an anchor for proper chromosomes separation (29, 30). Interestingly, we observed that the angle of the plane containing the two centrosomes to the plane of the adhesion surface (Figure 3 D) during metaphase is larger on average when the AA mutant is expressed. No such difference was observed with the DD mutant (Figure 3 E). This indicates that, at a given time during metaphase, the centrosomes are less likely to be on a plane parallel to the adhesion surface when AA mutant is expressed (Figure 3 F). In other words, it takes more time to align the centrosome in AA mutant-expressing cells, likely delaying anaphase onset. Thus, the double phosphorylation of Merlin appears necessary for mitosis to proceed and its absence delays the transition from NEB to SCS.

Phosphorylation of Merlin on S518 and T581 differentially inhibits binding to α-tubulin and Ezrin

Merlin was shown to bind and to destabilize microtubules (24). When we examined the binding of α-tubulin to GFP-Merlin, we observed a strong interaction during interphase that is nearly abolished during mitosis (Figure 4A). Importantly, we observed that the DD mutant weakly interacts with α-tubulin in contrast to the strong binding of the AA mutant (Figure 4B and Supplementary Figure 3A). This suggests that the phosphorylation of Merlin during mitosis inhibits the interaction of Merlin with microtubules. It was previously observed that phosphorylation of S518 decreases the affinity of Merlin for α-tubulin (23). We used single mutant (A or D) of S518 and T581 to investigate their respective role in regulating Merlin/α-tubulin binding. Interestingly, we found opposite effects. As expected 518A mutant bound much better than 518D. However, 581D mutant bound strongly to α-tubulin compared to 581A (Figure 4B and Supplementary Figure 3B). Thus it appears that the phosphorylation of S518 controls the interaction with α-tubulin. Merlin isoform 2 doesn't contain T581. We observed that it binds consistently better than isoform 1 to tubulin (Figure 4C). Nevertheless, the interaction is much weaker during mitosis (Figure 4D) and also when S518 is changed for an aspartic residue compared to an alanine, demonstrating the same mode of regulation for both isoforms (Figure 4E). The observation that Merlin mutant T581D binds α-tubulin better than T581A suggest that the former may harbor a different conformation making the FERM domain more accessible. This hypothesis is supported by the observation that isoform 2, which is expected to be under a more open conformation

resulting from the absence of interaction between the FERM and the C-ERMAD (C-terminal ERM association Domain) domains, also binds better to α-tubulin when compared to isoform 1. We then used co-immunoprecipitation assays between GST-Merlin-FERM and GFP-C-ter half of Merlin to test the effect of single and double phosphosite mutations on the intramolecular interaction (Figure 4F left panel). As observed by *Sher et al.* (31), S518D mutation tends to increase the interaction. In contrast, T581D strongly weakens intramolecular interaction suggesting that phosphorylation of T581 may open Merlin isoform 1 conformation. Dual DD and AA mutants showed barely any differences indicative of antagonistic effects. Merlin C-ERMAD also interacts with ERM FERM domain. Using the same strategy, we tested Merlin C-terminus interaction with Ezrin FERM domain (Figure 4F right panel). We did not observe a significant impact of S518 D or A mutation. However, the substitution of an alanine for T581 resulted in a dramatic increase in the interaction with Ezrin FERM domain when compared to aspartic acid substitution. Merlin AA mutant also bound better than the DD mutant indicating that phosphorylation of T581 is predominant for the regulation of Merlin/Ezrin interaction (Figure 4F right panel).

ERM binds α-tubulin via their FERM domain and the interaction stabilizes microtubules at the cell cortex in the case of Moesin (19). We investigated if Merlin C-terminal domain may interfere with the binding of α-tubulin to the FERM domain of Ezrin. α-tubulin was coprecipitated with GFP-Ezrin in the presence or absence of Merlin C-terminal AA domain. As expected, Merlin C-terminal AA domain co-immunoprecipitated with GFP-Ezrin (Figure 5A). Interestingly, its expression stimulated the binding of α-tubulin to GFP-Ezrin. Actin binding to Ezrin was also stimulated under these conditions. Actin binds to the C-terminal end of Ezrin and our result suggests that the interaction of Merlin C-terminal domain with Ezrin may lead to a change in Ezrin conformation, exposing both the FERM and C-terminal domains for interaction (Figure 5A).

To better understand the dynamics of Merlin and Ezrin mutual interaction and with α-tubulin during mitosis, we evaluated their phosphorylation state during M to G1 transition following nocodazole block release in Hela cells. The re-entry into G1 was followed by FACS (Figure 5B) and the progression from metaphase to anaphase and telophase was followed by immunofluorescence and DAPI staining. We noticed that the kinetics of phosphorylation of S518 and T581 of Merlin are different. S518 phosphorylation shows a pronounced decrease at the onset of anaphase and upon G1 entry and parallels Aurora A expression. T581 phosphorylation dropped later corresponding to G1 entry. This could be a direct consequence of our observation showing that the phosphorylation of S518 facilitates T581 modification. In contrast, T567 phosphorylation of Ezrin, that leads to a more open conformation, was low in metaphase but reached a maximum 2 hours after release, corresponding to a strong enrichment of cells in telophase. Then, the signal decreased strongly upon G1 entry (Figure 5B). It is well established that T567 phosphorylation of Ezrin stimulates its binding to actin (32) but the impact on α–tubulin interaction was not clearly defined. Using GFP-Ezrin mutants harboring either T567 D or A substitutions, we coprecipitated actin from HEK293 cells. We clearly confirmed the increased binding of actin to the T567D mutant. Interestingly, no difference was observed between A and D mutant for the binding to α-tubulin (Figure 5C right panels). We also confirmed the increased interaction of Ezrin with actin during mitosis (metaphase), using GFP trap. However, the same experiment showed a reproducible concomitant decrease in α-tubulin binding (Figure 5C left panels). In the end, we observed that actin binding to Ezrin was maximum two hours after nocodazole release (Figure 5D), likely a consequence of elevated T567 phosphorylation whereas α-tubulin interaction was rather low during mitosis and increased upon G1 entry, possibly resulting from increased binding of Merlin to the FERM domain of Ezrin. Our results thus show how phosphorylation events dynamically modulate Merlin and Ezrin interactions with α-tubulin and actin, necessary for mitosis progression, either directly or indirectly.

Several NF2 patient mutations alter Merlin phosphorylation and α-tubulin binding

We next investigated if *NF2* mutations identified in patients could modify Merlin phosphorylation on S518 and T581 and its binding to α-tubulin. We found that T581 phosphorylation was not affected by the mutations tested (Figure 6A). On the contrary, S518 phosphorylation was abolished in ∂2-3 (lane3 and also Figure 1 I) and L64P mutants (lane 13), and reduced in K79E and Q324L (lane 4 and 5) when compared to isoform 1 (all mutants are from isoform 1). Interestingly, this phosphorylation was consistently higher in isoform 1 than in isoform 2 (lane 1 and 2). We observed that mutants Q324L and L64P displayed increased tubulin binding (lane 5 and 13). As expected, the C-terminal half of Merlin showed no α-tubulin binding (lane 19). It also showed no phosphorylation on S518, which was expected since the binding region for Aurora A, like PAK1 is localized in the FERM domain (4). Of interest, the absence of T581 phosphorylation suggests that the kinase binding site is also located in the N-terminal half of Merlin. Mutations that would result in C-terminal truncation tended to decrease α-tubulin binding (M1-480 and M1-532 lanes 17 and 18). However, the sequence M1-330 corresponding to the FERM domain displayed higher binding than the full lengh Merlin likely due to the absence of masking from the C-terminal sequence. Finally, we tested the impact of L64P and Q324L mutants on mitosis duration because both of them showed elevated α-tubulin binding. Q324L slightly shortened mitosis but L64P slowed mitosis to a similar extent as Merlin AA mutant (Figure 6B and Supplementary Figure 4). In addition, upon L64P expression, about 13% of cells that started mitosis were unable to reach telophase after several hours and died. These results suggest that both α-tubulin binding and S518 dephosphorylation are required to induce a delay in mitotic progression. However, we cannot exclude that these mutations of Merlin eventually delay mitosis progression by other mechanisms.

Thus, we confirm that several NF2 patient mutations alter Merlin phosphorylation state and α-tubulin binding. Although the two events appear largely independent in this case, our data indicate that the expression of a subset of mutants of Merlin found in patients is likely to interfere with mitotic progression.

Discussion

The major function of Merlin is to inhibit cell proliferation, notably in response to cell-cell contacts. Most studies have shown that Merlin exerts its tumor suppressor role primarily by inhibiting important mitogenic signaling pathways (33-38). However, some recent evidences of its implication in cell cycle progression have emerged. In this report, we show that Merlin phosphorylation is likely necessary for a proper progression from metaphase to anaphase and correct spindle positioning. This could be due to its capacity to modulate Merlin interaction with α-tubulin. Indeed, Merlin was reported to bind to microtubules, promoting their stabilization (24) but the functional consequences were not explored. During mitosis, Merlin could play a role analogous to Ezrin which binding to α-tubulin stabilizes aster microtubules ensuring correct positioning of the centrosomes (21). A role for Merlin during mitosis was also proposed although through a very different mechanism. *Hebert et al*. showed that Merlin restricts Ezrin cortical distribution so that, upon activation during mitosis, Ezrin directs the correct positioning of the centrosomes and proper orientation of mitotic spindles (18) necessary for the establishment of epithelial architecture. Thus, Merlin may influence mitotic progression by modulating Ezrin functions. Interestingly, it was also reported that a correct polarized localization of NuMa is necessary for proper spindle orientation in mitosis and requires the local activation of Ezrin by the Slk kinase (39). The expression of a constitutively active form of Ezrin leads to an unpolarized recruitment of NuMa and a defect in spindle orientation in mouse apical progenitor, resulting in the same spindle orientation defect that we observed in Hela cells expressing the Merlin AA mutant. The expression of Merlin AA mutant stimulates the interaction of Ezrin with α-tubulin and actin, equivalent to the activation of Ezrin by phosphorylation. It is thus conceivable that Merlin AA expression induces an unpolarized activation of Ezrin perturbing NuMa recruitment and leading to spindle misorientation. However, the alteration of the binding of α-tubulin and actin to Ezrin induced by Merlin AA might also be involved in the phenotype.

Hence, our results indicate that Merlin likely plays an important role during cell division through distinct mechanisms. They underline the importance of the interplay between Merlin and Ezrin for a proper progression of mitosis that was suggested in other studies (18, 40).

In addition, we observed that several patient mutations lead to altered phosphorylation of Merlin and tubulin binding. The two effects, however, were not necessarily linked. This suggests that the mutations also likely induce changes in Merlin conformation independently affecting the binding of the kinase and to α-tubulin. Thus, in contrast to WT Merlin, specific mutants can still bind to α-tubulin and Ezrin during mitosis and could act as a gain of function mutants inducing a delay in mitotic progression. Interestingly, such delays were previously linked to an increased risk of DNA damage by various mechanisms (41). They usually lead to genomic instability and favor either tumorigenesis or apoptosis. Point mutations have in general been linked to milder forms of NF2 (42-44) and our results thus support the idea that mutations disturbing Merlin phosphorylation in mitosis trigger cell death and protect from tumor development to a certain point. This seems to be the case for the L64P mutant which strongly delays mitosis completion and induces cell death in a large subset of mitotic cells. It would be of interest to know if L64P mutants are associated to a milder for of the disease. However, severe phenotypes associated to point mutations were also reported (45) indicating that the outcome is linked to the nature of the mutation.

Several studies reported that isoform 2 does not inhibit cell proliferation (46) conflicting with other publications (47-49). Mice engineered to express either isoform 1 or 2 both developed normaly and were protected from tumor development (50) demonstrating their functional redundancy. Nevertheless, the same study reported functionnal differences, as isoform 2 was uniquely involved in the maintenance of axonal integrity. We uncovered a new phosphorylation site that is specific to isoform 1. T581 phosphorylation abolishes Merlin C-terminal interaction with Ezrin FERM domain and promotes Merlin binding to α-tubulin. It also decreases Merlin head to tail interaction (Figure 4F) and is more likely to participate in Merlin open conformation than S518 phosphorylation, in coherence with results reported recently (51, 52) Interestingly this phosphorylation confers to isoform 1 interaction properties that are similar to those of isoform 2. Indeed, isoform 2 doesn't interact with Ezrin Ferm domain via its C-terminal end and binds more efficiently to α-tubulin than isoform 1 via its FERM domain. Hence, during mitosis, T581 phosphorylation prevents Merlin 1/Ezrin interaction while Merlin 2 is not interacting anyway. However, this modification alone would promote tubulin binding but is superseded by S518 phosphorylation which inhibits this interaction for both isoforms. Thus, our results show that soform I have additional means of regulating its binding to specific molecular partners, compared to isoform 2. In summary, although isoform 1 and 2 exert essentially the same molecular functions, these can be differentially regulated by phosphorylation depending on the cellular context. This could explain the absence of functional redundancy that was sometimes observed in cells and mice when both isoforms are expressed.

In summary, we have uncovered a potential novel function of Merlin as a regulator of mitotic progression. Merlin is a bona fide substrate for the mitotic kinase Aurora A. Its phosphorylation and subsequent release from microtubules and from Ezrin appear to be required for mitosis to proceed correctly (Figure 7). Our results suggest that, in wild-type cells, specific mutations on a single allele of *NF2* could result in the production of a Merlin mutant with altered phosphorylation and binding to α–tubulin and Ezrin acting dominantly and influencing the early stages of tumorigenesis. It would be of great interest to evaluate how the severity of the disease is linked to the capacity of a point mutation to alter Merlin function during mitosis. However, the rarity of the disease and the diversity of *NF2* mutations may render this study difficult to perform.

Experimental procedures

Plasmids constructs: GFP-Merlin expression vectors were constructed by inserting the cDNA of

isoform 1, 2 and patients derived mutants (kindly provided by Joseph Kissil, Scripps Research Institute, Florida) into pEGFPC1 (Clonetech).

Cell culture: Human embryonic kidney (HEK293) cells and Hela cells were cultured in DMEM medium supplemented with 10% FBS, penicillin (500 units/mL) and streptomycin (500 µg/ml) antibiotics (all Gibco, Life technologies, France) at 37°C with 5% CO_2.

Inducible cell lines: Hela cell lines inducible expressing Merlin mutants were generated using the RetroX Tet On advanced inducible system (Clonetech) following manufacturer guidelines. The expression of Merlin mutants was confirmed by immunofluorescence.

Cell synchronization in mitosis and drug treatments: Following 16h treatment with 0.5µg/ml Nocodazole, mitotic Hela cells were detached and collected by shaking the plate, Cells still attached represented the interphasic fraction. The Aurora A and B inhibitors (MLN8054, ZN4474, Sigma-Aldrich) were added at 1 µg/ml for 1 hour to the culture media of cell blocked in mitosis with nocodazole. MG132 was added at 1 µM to prevent exit from mitosis.

Timelapse and mitosis duration experiments: Hela inducible cells were plated in DMEM+10%FBS with or without Doxycycline 1µg/ml, in 3 cm Fluorodish (World Precision Instruments). Video acquisition started 8h after release from a 16h block in S phase with 2mM thymidine (with or without doxycycline) at 37°C, and 5% CO2 with Nikon video microscope using 40X (NA 1.3) DIC oil objective and binning2. One image was taken every 2 min for 20h. For each experiment, 2 to 4 acquisitions were sequentially performed for each condition (+ or - doxycycline) and the data were pooled. Video analysis was done with ImageJ software and duration was calculated with tracking plugin.

Measurements of angles during metaphase: Fixed metaphasic cells overexpressing or not mutant Merlin AA (39 cells) or DD (43 cells) were stained for Merlin, α-tubulin and DNA (DAPI). Images were acquired with a Zeiss Axio-observer Z1 microscope, controlled by axiovision software and with a Hammatsu Camera using a 63X immersion oil objective, 1.40 plan apo and 1.6 optovar and binning1. Voxels were collected at 64nm lateral and 240nm axial intervals, followed by deconvolution using the Huygens software. The distance between the planes containing the centrosomes (in µm) was calculated as $\Delta z=n*0,24$ were n is the number of focal planes separating the two centrosomes. The angle of the plane containing the centrosomes to the adhesion plane was calculated as $a=\arctan(\Delta z/d)$ were d is the projected distance between the two centrosomes (in µm). Measurements were made with Icy software.

FACS analysis: Hela cells released from nocodazole block were fixed in paraformaldehyde 4% for 10 minutes followed by a permeabilization in PBS + 0.2% Triton X100 for 10 minutes, stained with DAPI at 1µg/ml and the DNA content was measure by FACS on a Guava EasyCyte flow cytometer (Merck Millipore). In parallel, a subset of cells were plated on coverslips, fixed and stained under the same conditions. Each timepoint was evaluated for enrichment in cells in metaphase or telophase to document the progression through mitosis using a Leica DM 6000B epifluorescence microscope and a 63X (NA 1.4) oil immersion objective.

Immunofluorescence and microscopy: Cells were seeded seeded on glass coverslips and fixed in 4% paraformaldehyde for 10 minutes followed by a permeabilization in PBS + 0.2% Triton X100 for 10 minutes. Incubation with primary antibody was done in PBS + 0.1% Tween 20 + 10 % FBS, overnight at +4C. The secondary antibodies were incubated in the same buffer for 2 hours at room temperature together with DAPI at 1µg/ml. Images were acquired on a Leica DM 6000B epifluorescence microscope and a 40X (NA 1.3) or a 63X (NA 1.4) oil immersion objective.

GFP trap: Cell lysates were prepared and incubated overnight with GFP-Trap beads (ChromoTek, Deutschland) following manufacturer's instructions.

Western-blotting and quantification: Between 20 to 40µg of protein extracts were loaded on NuPage 4-12% bis-tris gels in MES migration buffer (Invitrogen). The transfer was performed using Iblot gel transfer stack Nitrocellulose (Invitrogen). Membrane were usually blocked with 5% low fat milk in Tris Buffered Saline plus 0,5% Tween20 Buffer (TBST) for 20 minutes. Primary antibody was incubated with the membrane overnight at +4°C in TBST+10%FBS. Following three 10 minutes rinses in TBST, the membranes were incubated with secondary Horse radish peroxidase (HRP) labelled antibodies (Amersham) for one hour at room temperature. After three additio~~n~~nal 10 minutes rinses in TBST, the membranes were incubated with develo~~p~~ping solution (SuperSignal West Pico, Thermofisher). Then, signal intensities of blotting images were analyzed by imaging software (Bio-Rad Image lab v 4.0.1) using manufacturer's procedure. Briefly, the same size of pixel area was selected and signal intensity calculated by subtraction the background signal. Each signal was normalized with reference to standard control signals, e.g. actin or total protein (when analyzed for phospho-proteins), and a signal/control ratio was calculated.

Antibodies: Ezrin antibody was a kind gift from Monique Arpin. Cell Signaling: Aurora A (14475), phospho Aurora A T288 (2914), phospho Aurora B T232 (2914), phospho Ezrin T567 (3141). Santa Cruz: Merlin (C-18 SC-332 and N-19 SC-331), GFP (SC-8334 and SC-9996) Sigma: actin (A2228), α-tubulin (T9026). Rockland: phospho Merlin S518 (600-401-414). Covalab (Lyon, France): Merlin (pab0939p).

Generation of pT581 Merlin antibody: The AERTYGDVERA peptide phosphorylated on the threonine was coupled to albumin. Rabbit immunization and purification against phosphorylated and non-phosphorylated peptides were done by Covalab (Lyon, France).

Merlin in vitro phosphorylation assay: GFP-Merlin WT and S518A immunoprecipitated by GFP Trap from HEK293 were treated with 50 units of Calf Intestinal Alkaline Phosphatase (Biolabs) at 30°C for 2 hours in phosphatase buffer and washed 3 times with kinase buffer. One microgram~~me~~ of purified Aurora A kinase (Millipore, 14-511) was added to the beads for one hour at 30°C. The reaction was stopped with Laemmli buffer at 95°C for 10 minutes.

Proteomics and Mass spectrometry: GFP tagged Merlin was immunoprecipitated from HEK293, separated by SDS-PAGE and visualized with commassie staining, after which the protein bands were cut out from the gel, digested with trypsin into peptides, and analyzed by liquid chromatography–tandem mass spectrometry (LC-MS/MS) using an Ultimate 3000 nano-LC (Dionex, Sunnyvale, CA) coupled to an LTQ Orbitrap XL mass spectrometer (Thermo scientific/MDS Sciex, Foster City, CA). The fragmentation spectrum is derived from a tryptic (1 missed cleavage) Merlin peptide.

In vitro Merlin/Ezrin and Merlin/Merlin interactions: GFP tagged Merlin constructs precipitated from HEK293 by GFP trap were incubated for 3h at 4°C with his tagged purified Ezrin FERM domain or purified GST Merlin. After 6 rinses in lysis buffer (20mM Hepes, 100mM NaCl, 0.5mM EDTA, 0.1% tritonX100, PIC 1/100 Sigma), beads were resuspended in loading buffer and protein complex were analyzed by western-blot.

Acknowledgements

We are grateful to Fatima Mechta-Grigoriou for her help and constant support. We would like to thank Alizée Boin and Christophe Couderc for stimulating discussions. We are thankful to Olivier Gavet, Veronique Marthens, Dora Sabino and Renata Basto for useful advices and sharing reagents. We wish to thank the imaging facilities from Curie Institute (Nikon Imaging Center) and Imagif. VM was supported by the Pierre Gilles de Gennes Foundation. The project was supported by funds from Association pour la

Recherche sur le Cancer (ARC), Association Neurofibromatose et Recklinghausen (ANR) and Institut National du Cancer (INCA), Centre Nationale de la Recherche Scientifique (CNRS), Institut National de la Sante et de la Recherche Médicale (INSERM) and Institut Curie.

Conflict of interest: The authors declare that they have no conflicts of interest with the contents of this article.

References

1. Lallemand, D., Curto, M., Saotome, I., Giovannini, M., and McClatchey, A.I. (2003). NF2 deficiency promotes tumorigenesis and metastasis by destabilizing adherens junctions. *Genes Dev*. 17, 1090– 1100

2. McClatchey A.I., Saotome I., Ramesh V., Gusella J.F., Jacks T. (1997) The Nf2 tumor suppressor gene product is essential for extraembryonic development immediately prior to gastrulation. *Genes & Dev*. 11, 1253–1265

3. Giovannini M., Robanus-Maandag E., van der Valk M., Niwa-Kawakita M., Abramowski V., Goutebroze L., Woodruff J.M., Berns A., Thomas G.(2000) Conditional biallelic Nf2 mutation in the mouse promotes manifestations of human neurofibromatosis type 2. *Genes & Dev*. 14,1617–1630

4. Kissil JL, Wilker EW, Johnson KC, Eckman MS, Yaffe MB, Jacks T. (2003). Merlin, the product of the Nf2 tumor suppressor gene, is an inhibitor of the p21-activated kinase, Pak1. *Mol Cell* 12, 841–849

5. Tikoo, A., Varga, M., Ramesh, V., Gusella, J., and Maruta, H. (1994). An anti-Ras function of neurofibromatosis type 2 gene product (NF2/Merlin). *J. Biol. Chem*. 269, 23387–23390

6. Morrison H, Sperka T, Manent J, Giovannini M, Ponta H, Herrlich P. (2007). Merlin/neurofibromatosis type 2 suppresses growth by inhibiting the activation of Ras and Rac. *Cancer Res*. 67, 520–527

7. James, M.F., Han, S., Polizzano, C., Plotkin, S.R., Manning, B.D., Stemmer-Rachamimov, A.O., Gusella, J.F., and Ramesh, V. (2009). NF2/merlin is a novel negative regulator of mTOR complex 1, and activation of mTORC1 is associated with meningioma and schwannoma growth. *Mol. Cell. Biol.* 29, 4250–4261

8. Maitra, S., Kulikauskas, R.M., Gavilan, H., and Fehon, R.G. (2006). The tumor suppressors Merlin and Expanded function cooperatively to modulate receptor endocytosis and signaling. *Curr. Biol*. 16, 702–709

9. Lallemand, D., Manent, J., Couvelard, A., Watilliaux, A., Siena, M., Chareyre, F., Lampin, A., Niwa-Kawakita, M., Kalamarides, M., and Giovannini, M. (2009). Merlin regulates transmembrane receptor accumulation and signaling at the plasma membrane in primary mouse Schwann cells and in human schwannomas. *Oncogene* 28, 854–865

10. Li, W., You, L., Cooper, J., Schiavon, G., Pepe-Caprio, A., Zhou, L., Ishii, R., Giovannini, M., Hanemann, C.O., Long, S.B., Erdjument-Bromage, H., Zhou, P., Tempst, P. and Giancotti FG. (2010). Merlin/NF2 suppresses tumorigenesis by inhibiting the E3 ubiquitin ligase CRL4(DCAF1) in the nucleus. *Cell* 140, 477–490

11. Zhang, N., Bai, H., David, K.K., Dong, J., Zheng, Y., Cai, J., Giovannini, M., Liu, P., Anders, R.A., and Pan, D. (2010). The Merlin/NF2 tumor suppressor functions through the YAP oncoprotein to regulate tissue homeostasis in mammals. *Dev. Cell* 19, 27–38

12. Su T., Ludwig M.Z., Xu J., Fehon R.G. (2017). Kibra and Merlin Activate the Hippo Pathway Spatially Distinct from and Independent of Expanded. *Dev Cell.* 40, 478-490.

13. Li W, Cooper J, Zhou L, Yang C, Erdjument-Bromage H, Zagzag D, Snuderl M, Ladanyi M, Hanemann CO, Zhou P, Karajannis MA, Giancotti FG. (2014) Merlin/NF2 loss-driven tumorigenesis linked to CRL4(DCAF1)-mediated inhibition of the hippo pathway kinases Lats1 and 2 in the nucleus. *Cancer cell* 26(1), 48-60

14. Boin A, Couvelard A, Couderc C, Brito I, Filipescu D, Kalamarides M, Bedossa P, De Koning L, Danelsky C, Dubois T, Hupé P, Louvard D, Lallemand D. (2014). Proteomic screening identifies a YAP-driven signaling network linked to tumor cell proliferation in human schwannomas. *Neuro Oncol.* 16(9), 1196-209.

15. Guerrant W, Kota S, Troutman S, Mandati V, Fallahi M, Stemmer-Rachamimov A and Kissil J. (2016). YAP Mediates Tumorigenesis in Neurofibromatosis Type 2 by Promoting Cell Survival and Proliferation through a COX-2-EGFR Signaling Axis. *Cancer Research* 76:3507–3519.

16. Muranen, T., Grönholm, M., Renkema, G.H., and Carpén, O. (2005). Cell cycle-dependent nucleocytoplasmic shuttling of the neurofibromatosis 2 tumour suppressor merlin. Oncogene 24, 1150–1158

17. Grönholm, M., Muranen, T., Toby, G.G., Utermark, T., Hanemann, C.O., Golemis, E.A., and Carpén, O. (2006). A functional association between merlin and HEI10, a cell cycle regulator. *Oncogene* 25, 4389–4398

18. Hebert, A.M., DuBoff, B., Casaletto, J.B., Gladden, A.B., and McClatchey, A.I. (2012). Merlin/ERM proteins establish cortical asymmetry and centrosome position. *Genes Dev.* 26, 2709–2723

19. Carreno, S., Kouranti, I., Glusman, E.S., Fuller, M.T., Echard, A., and Payre, F. (2008). Moesin and its activating kinase Slik are required for cortical stability and microtubule organization in mitotic cells. J. *Cell Biol*. 180, 739–746.

20. Kunda, P., Pelling, A.E., Liu, T., and Baum, B. (2008). Moesin controls cortical rigidity, cell rounding, and spindle morphogenesis during mitosis. *Curr. Biol*. 18, 91–101

21. Solinet S., Mahmud K., Stewman S.F., Ben El Kadhi K., Decelle B., Talje L. Ma A., Kwok B.H., and Carreno S. (2013). The actin-binding ERM protein Moesin binds to and stabilizes microtubules at the cell cortex. *J. Cell Biol.* 202(2), 251–260

22. Machicoane M., de Frutos C.A., Fink J., Rocancourt M., Lombardi Y., Garel S., Piel M. and Echard A. (2014). SLK-dependent activation of ERMs controls LGN–NuMA localization and spindle orientation J. *Cell Biol.* 205(6), 791–799

23. Muranen T., Gronholm M., Lampin A., Lallemand D., Zhao F., Giovannini M. and Carpen O. (2007). The tumor suppressor merlin interacts with microtubules and modulates Schwann cell microtubule cytoskeleton. *Human Molecular Genetics*, 2007, 16(14), 1742–1751

24. Smole Z, Thoma CR, Applegate KT, Duda M, Gutbrodt KL, Danuser G. and Krek K.(2014) Tumor Suppressor NF2/Merlin Is a Microtubule Stabilizer. *Cancer Res.* 74:353-362

25. Kettenbach A.N1, Schweppe D.K., Faherty B.K., Pechenick D., Pletnev A.A. and Gerber S.A. (2011) Quantitative phosphoproteomics identifies substrates and functional modules of Aurora and Polo-like

kinase activities in mitotic cells. *Sci Signal* 4(179): 10.1126/scisignal.2001497.

26. Giovannini, M., Robanus-Maandag, E., Niwa-Kawakita, M., van der Valk, M., Woodruff, J.M., Goutebroze, L., Mérel, P., Berns, A., and Thomas, G. (1999). Schwann cell hyperplasia and tumors in transgenic mice expressing a naturally occurring mutant NF2 protein. *Genes & Dev*. 13, 978–986

27. Yabuta N., Mukai S., Okada N., Aylon Y., Nojima H. The tumor suppressor Lats2 is pivotal in Aurora A and Aurora B signaling during mitosis. (2011). *Cell Cycle*. 10(16):2724-36.

28. Laulajainen, M., Muranen, T., Nyman, T.A., Carpén, O., and Grönholm, M. (2011). Multistep phosphorylation by oncogenic kinases enhances the degradation of the NF2 tumor suppressor merlin. *Neoplasia* 13, 643–652

29. Reboutier D., Benaud C. and Prigent C. (2015) Aurora A's Functions During Mitotic Exit: The Guess Who Game. Front Oncol. 5: 290

30. Gavet O. and Pines J. (2010) Progressive Activation of CyclinB1-Cdk1 Coordinates Entry to Mitosis. *Dev Cell.* 18, 533–543

31. Sher I., Hanemann C.O., Karplus P.A. and Bretscher A. (2012). The tumor suppressor merlin controls growth in its open state, and phosphorylation converts it to a less-active more-closed state. *Dev. Cell* 22(4),703-5

32. Fievet BT, Gautreau A, Roy C, Del Maestro L, Mangeat P, Louvard D and Arpin, M. (2004). Phosphoinositide binding and phosphorylation act sequentially in the activation mechanism of ezrin. *J Cell Biol.* 164(5): 653–659.

33. Li W., Cooper J., Karajannis M.A. and Giancotti F.G. (2012) Merlin: a tumour suppressor with functions at the cell cortex and in the nucleus. *EMBO reports* 13(3), 204-215

34. Lopez-Lago M.A., Okada T., Murillo M.M., Socci N. and Giancotti F.G. (2009) Loss of the tumor suppressor gene NF2, encoding merlin, constitutively activates integrin-dependent mTORC1 signaling. *Mol Cell Biol.* 29, 4235–4249

35. Fehon R.G., McClatchey A.I. and Bretscher A. (2010) Organizing the cell cortex: the role of ERM proteins. *Nat Rev Mol Cell Biol.* 11, 276–287

36. Pan D. (2010) The Hippo signaling pathway in development and cancer. Dev Cell. 19, 491–505

37. Pellock, B.J., Buff, E., White, K., and Hariharan, I.K. (2007) The *Drosophila* tumor suppressors Expanded and Merlin differentially regulate cell cycle exit, apoptosis, and Wingless signaling. *Dev. Biol*. 304, 102–115.

38. Moleirinho S, Hoxha S, Mandati V, Curtale G, Troutman S, Ehmer U and Kissil, J. (2016). Regulation of localization and function of the transcriptional co-activator YAP by angiomotin. *eLife*. 6:e23966.

39. Kschonsak YT, Hoffmann. Activated ezrin controls MISP levels to ensure correct NuMA polarization and spindle orientation**.** J Cell Sci. 2018 May 21;131(10).

40. Meng J.J., Lowrie D.J., Sun H., Dorsey E., Pelton P.D. and Bashour A.M. (2000) Interaction between two isoforms of the NF2 tumor suppressor protein, Merlin, and between Merlin and ezrin, suggests modulation of ERM proteins by Merlin. *Neurosci Res.* 62(4), 491-502

41. Ganem N.J. and Pellman D. (2012) Linking abnormal mitosis to the acquisition of DNA damage. *J Cell Biol.* 199(6), 871-81

42. Kluwe L1. and Mautner V.F. (1996) A missense mutation in the NF2 gene results in moderate and mild clinical phenotypes of neurofibromatosis type 2. *Human Genet.* 97(2), 224-7

43. Ruttledge M.H1., Andermann A.A., Phelan C.M., Claudio J.O., Han F.Y., Chretien N., Rangaratnam S., MacCollin M., Short P., Parry D., Michels V., Riccardi V.M., Weksberg R., Kitamura K., Bradburn J.M., Hall B.D., Propping P. and Rouleau G.A. (1996) Type of mutation in the neurofibromatosis type 2 gene (NF2) frequently determines severity of disease. *Am J Hum Genet.* 59(2), 331-42

44. Baser M.E1., Friedman J.M., Aeschliman D., Joe H., Wallace A.J., Ramsden R.T. and Evans D.G. (2002) Predictors of the risk of mortality in neurofibromatosis 2. *Am J Hum Genet.* 71(4), 715-23

45. Scoles D.R1., Baser M.E. and Pulst S.M. (1996) A missense mutation in the neurofibromatosis 2 gene occurs in patients with mild and severe phenotypes. *Neurology* 47(2), 544-6

46. Sherman L., Xu H.M., Geist R.T., Saporito-Irwin S., Howells N., Ponta H., Herrlich, P. and Gutmann, D. H. (1997). Interdomain binding mediates tumor growth suppression by the NF2 gene product. *Oncogene* 15, 2505-2509

47. Lallemand D., Saint-Amaux A.L. and Giovannini M. (2009) Tumor-suppression functions of merlin are independent of its role as an organizer of the actin cytoskeleton in Schwann cells. *J Cell Sci.* 122, 4141–4149.

48. Laulajainen M., Melikova M., Muranen T., Carpén O. and Grönholm M. (2012) Distinct overlapping sequences at the carboxy-terminus of merlin regulate its tumour suppressor and morphogenic activity. *J Cell Mol Med.* 16, 2161–2175.

49. Bretscher A., Edwards K. and Fehon R.G. (2002) ERM proteins and merlin: integrators at the cell cortex. *Nat Rev Mol Cell Biol.* 3, 586–599

50. Schulz A., Baader S.L., Niwa-Kawakita M., Jung M.J., Bauer R., Garcia C., Zoch A., Schacke S., Hagel C., Mautner V.F., Hanemann C.O., Dun X-P., Parkinson D.B., Weis J., Schröder J.M., Gutmann D.H., Giovannini M., Morrison H. (2013) Merlin isoform 2 in neurofibromatosis type 2-associated polyneuropathy. *Nat Neurosci.* 16, 426–433

51. Chinthalapudi K., Mandati V., Zheng J., Sharff A.J., Bricogne G., Griffin P.R., Kissil J., Izard T. (2018). Lipid binding promotes the open conformation and tumor-suppressive activity of neurofibromin 2. *Nat Commun*. 9(1):1338.

52. Xing W., Li M., Zhang F., Ma X., Long J., Zhou H. (2017). The conformation change and tumor suppressor role of Merlin are both independent of Serine 518 phosphorylation. *Biochem Biophys Res Commun*. 493(1):46-51.

Figure 1

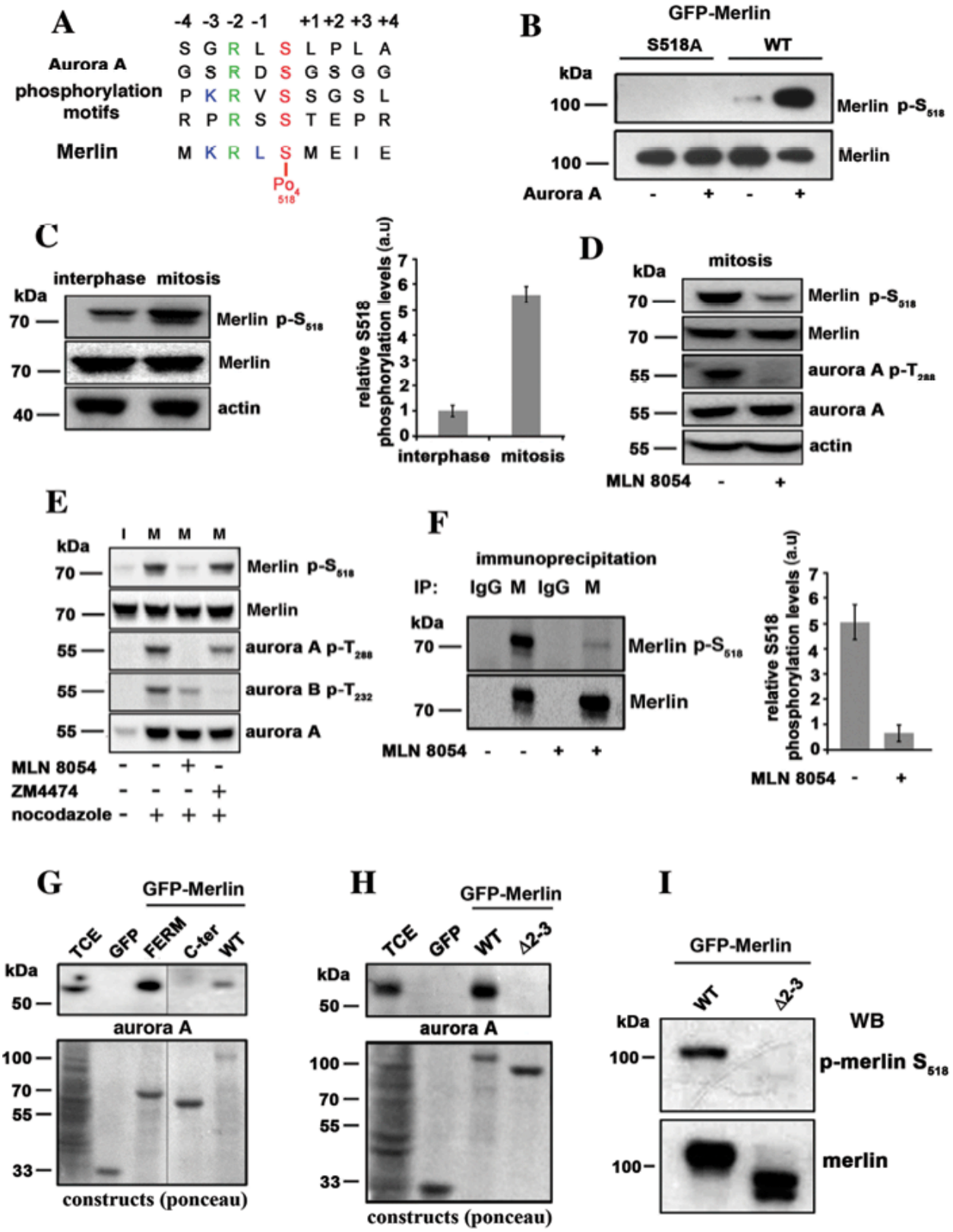

Figure 1: Merlin is a substrate for Aurora A on Serine 518 during mitosis. (**A**) The sequence of amino acids around serine 518 closely matches Aurora A target sequences. (**B**) GFP-Merlin (WT) and GFP-Merlin 518A were immunopurified from HEK293, dephosphorylated with alkaline phosphatase and incubated with recombinant Aurora A (+) or with the kinase buffer alone (-). The phosphorylation of S518 was detected using an antibody specific to the phosphorylated site. (**C**) The phosphorylation of S518 is higher in extracts from mitotic Hela cells overexpressing Merlin compared to interphasic cells. The quantification of 3 independent experiments is shown on the right graph (a.u= arbitrary units). (**D**) Mitotic Hela cells overexpressing Merlin were treated with the Aurora A inhibitor MLN 8054. The phosphorylation of Merlin on S518 and the activity of Aurora A (phosphorylation of T288) are strongly inhibited. (**E**) Mitotic (+ nocodazole) Hela cells overexpressing Merlin (M) were treated with Aurora A inhibitor (MLN8054) or Aurora B inhibitor (ZM4474) in the presence of MG132 proteasome inhibitor. Only MLN8054 inhibited phosphorylation on S518. Interphasic cell extract (I) is presented for comparison (- nocodazole). (**F**) Endogenous Merlin (M) was immunoprecipitated from extracts of mitotic HEK293 cells treated or not with MLN 8054. The samples were probed with antibodies to Merlin or p-Merlin S518. Non-specific antibody was use as a negative control (IgG). Quantification is presented on the right graph (3 experiments). (**G**) Co-immunoprecipitation using GFP fusion of Merlin full length (WT), Merlin Ferm domain (FERM, 1-330) or Merlin C-terminal half (330-595, C-ter) demonstrate that Merlin interacts with Aurora A via its Ferm domain. TCE-Total cell extract. (**H**) A patient mutant of Merlin Ferm domain skipping exon 2 and 3 (Δ2-3, aa 38 to 121) fails to bind to Aurora A as observed by co-immunoprecipitation. (**I**) Δ2-3mutant is not phosphorylated on S518 when expressed in mitotic Hela cells. Actin was used as loading control throughout. All blots shown above are representative of three independent biological experiments (n = 3). Error bars represent ±S.D.

Figure 2

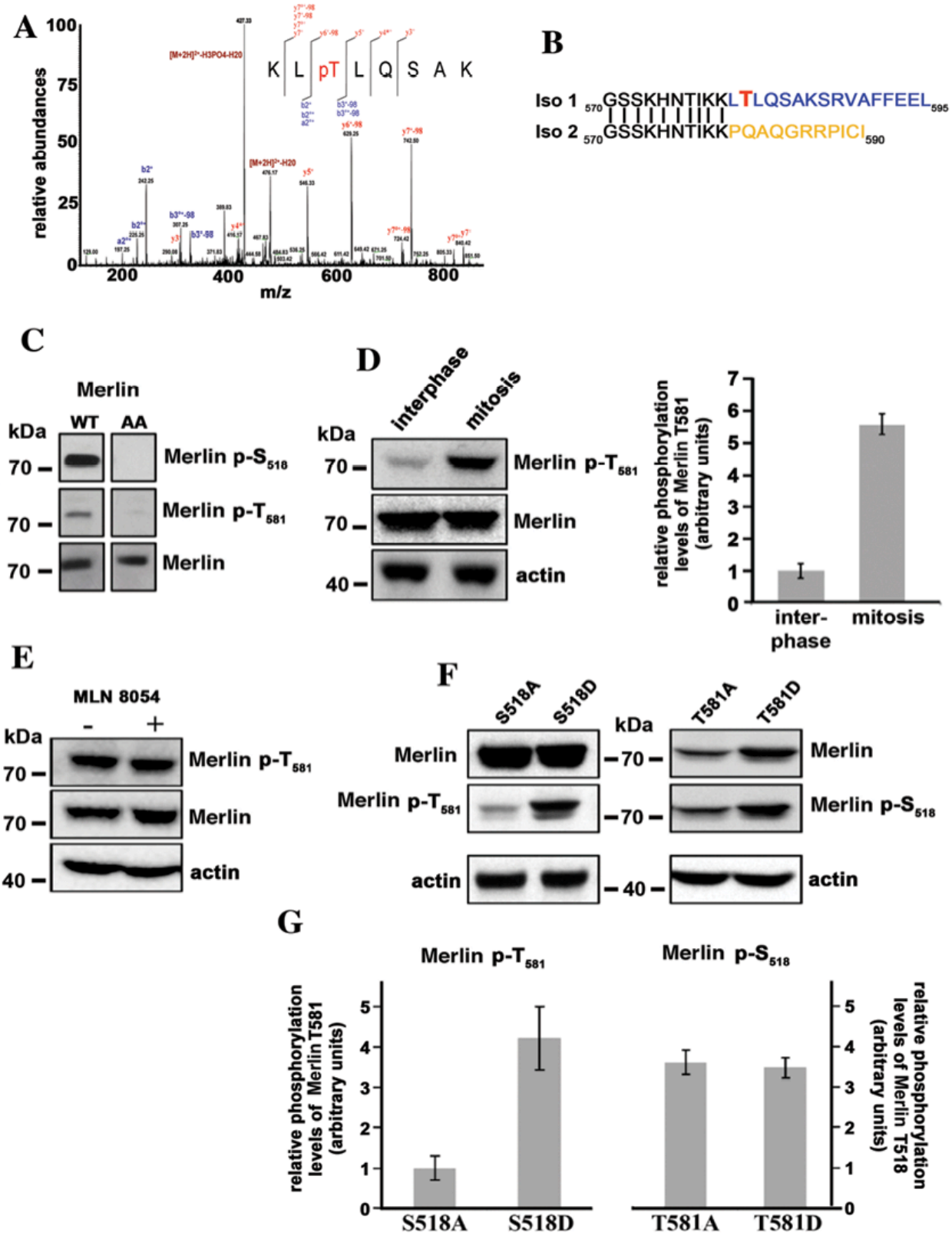

Figure 2: Threonine 581 of Merlin isoform 1 is phosphorylated during mitosis. (**A**) Mass spectrometry analysis of HEK293 cells overexpressing wild-type Merlin isoform 1 identifies a peak corresponding to a peptide phosphorylated on threonine 581. The peptide sequence and the observed ions of the phospho-peptide are shown with the spectrum. MS/MS spectrum is labeled to show singly charged b and y ions, as well as ion corresponding to neutral losses of water (o), NH3 (*) and H3PO4 group (98Da). LC-ESI MS/MS spectrum for peptide with the position of the phosphate group KLpT (581) LQSAK (484.762+ m/z). (**B**) The comparison of Merlin Isoform 1 and 2 sequences C-terminal to amino acid 570 show that T581 is unique to Isoform 1. (**C**) An antibody raised against a peptide including phospho-T581 recognizes Merlin overexpressed in HEK293 but doesn't recognized Merlin S518/T581A mutant (AA), proving good specificity. Specificity of the antibody to S518 was checked in parallel. (**D**) T581 is highly phosphorylated during mitosis in Hela cells overexpressing Merlin. The quantification of 3 independent experiments is shown on the right panel. (**E**) The treatment of mitotic Hela cells with MLN8054 has no impact on T581 phosphorylation. (**F**) The influence of alanine and aspartic substitutions of S518 or T581 on the phosphorylation level of the other site was evaluated by western-blot on extract from mitotic Hela cells. The S518A substitution clearly reduces the phosphorylation of T581 compared to S518D. There is no impact of T581A and D substitutions on S518 phosphorylation levels. (**G**) Quantification of 3 independent experiments corresponding to the conditions used in panel F. The ratio of phosphorylated Merlin to total Merlin is presented. Actin was used as loading control. All blots shown above are representative of three independent biological experiments (n = 3). Error bars represent ±S.D.

Figure 3

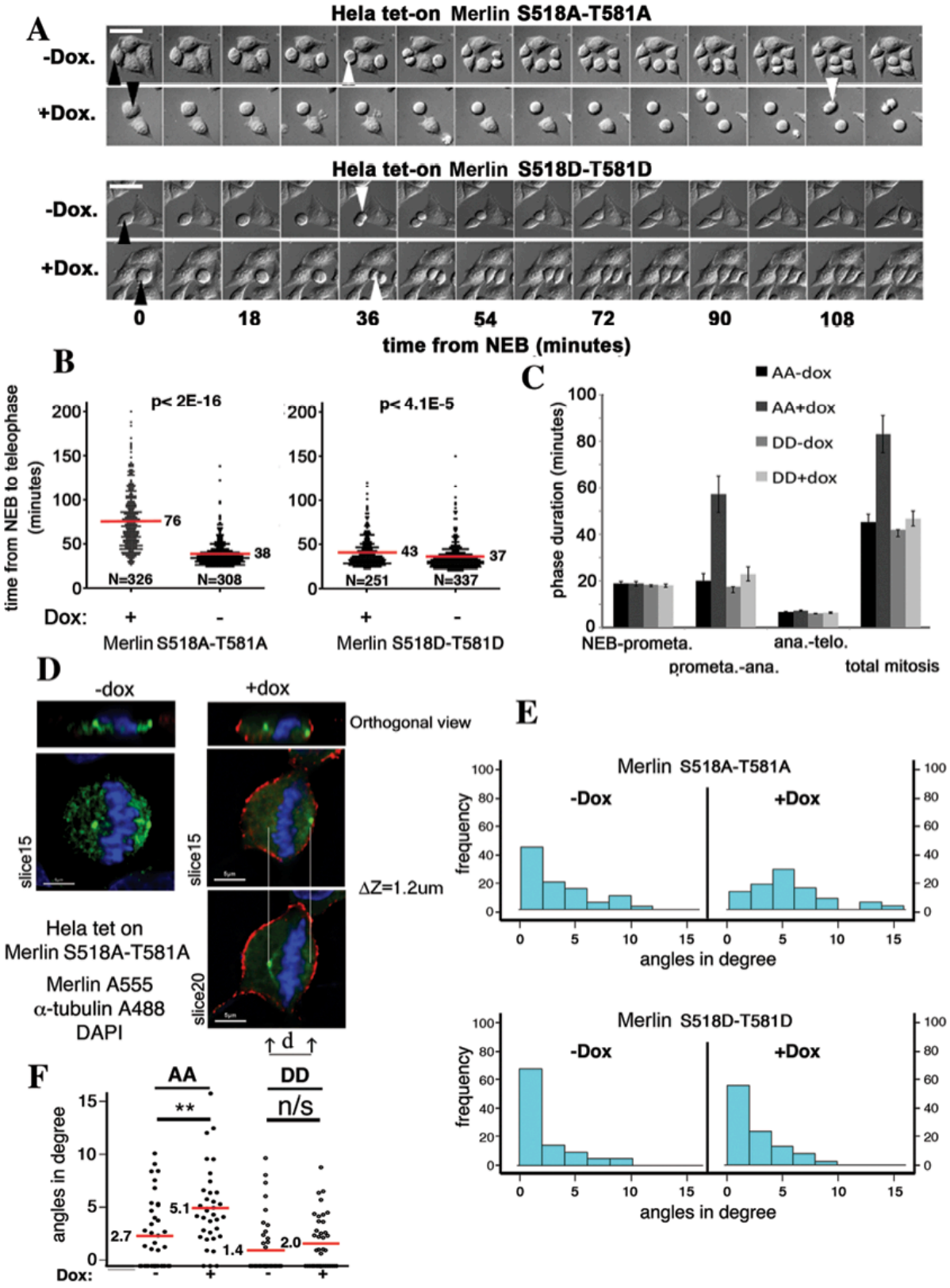

Figure 3: Phosphorylation of Merlin is necessary for mitotic progression. (**A**) The induced expression of a double alanine mutant of Merlin (S518A-T581A) strongly increases the interval between nuclear envelope breakdown (NEB, black arrowhead) and anaphase (white arrowhead) as observed by DIC microscopy. In contrast, the double aspartic mutant (S518D-T581D) doesn't. Size bar=30µm. The statistical analysis was done using Mann Whitney test on R Software. (**B**) The quantification of experiments such as presented in A shows that Merlin dual alanine mutant doubles the duration of NEB to anaphase. The induction of the phosphomimetic mutant has only a minor impact. (**C**) Phase contrast microscopy analysis reveals that mitotic delay is the result of a prolonged metaphase. (**D**) The angle of the plan going through the centrosome to the horizontal was measured during metaphase by combining α-tubulin staining and confocal microscopy on Merlin AA and DD overexpressing Hela cells. (**E**) The expression of Merlin AA but not Merlin DD mutant results in an increased frequency of higher angles. (**F**) Quantification of the average angle of the mitotic spindle plan to the horizontal in Hela cells shows a significant increase upon Merlin AA mutant expression. One-way ANNOVA: ns: $p>0.05$, *: $p<0.05$, **: $p<0.01$.

Figure 4

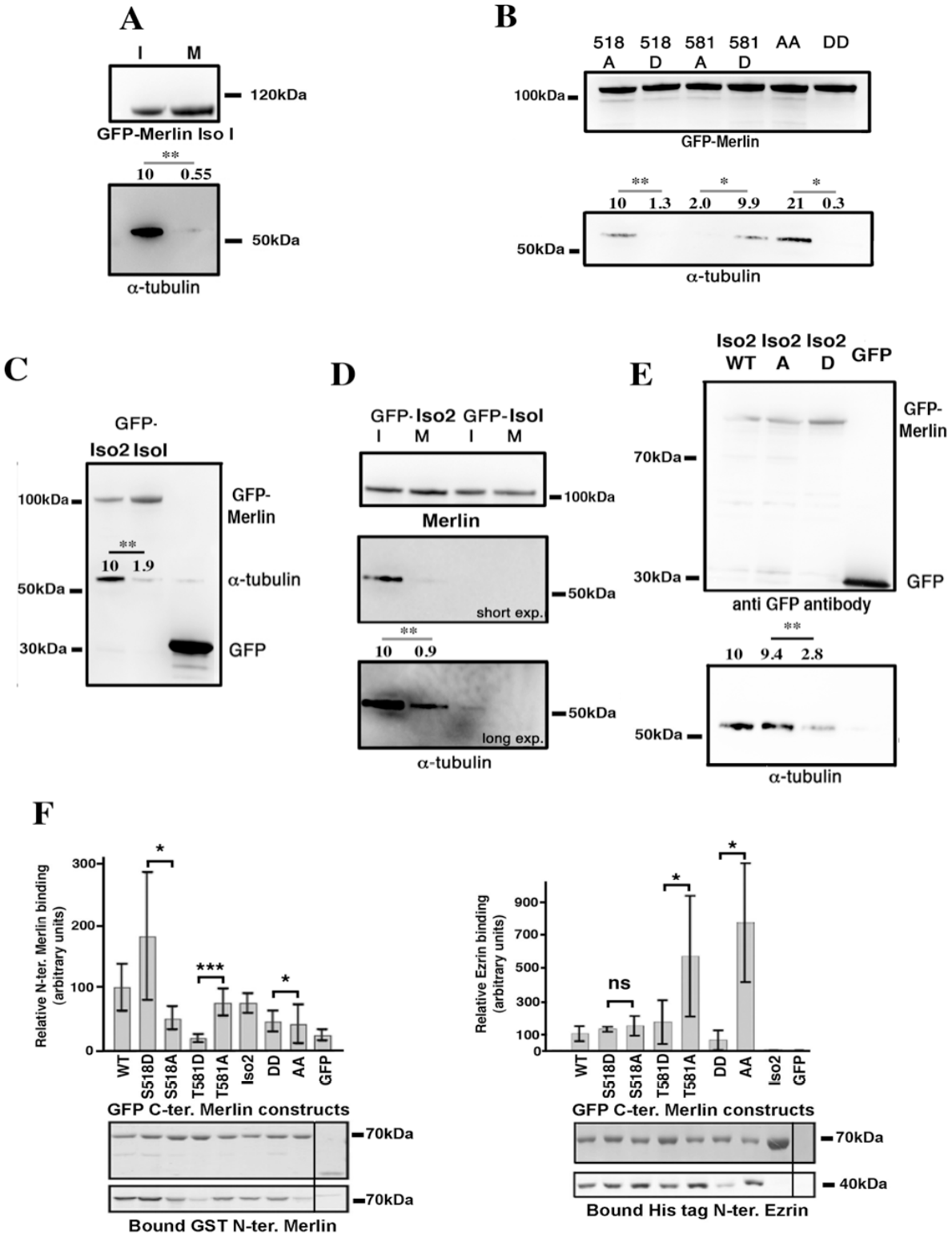

Figure 4: Phosphorylations of Merlin modulate its interaction with α-tubulin and with Ezrin. (**A**) In Hela cells, α-tubulin coprecipitate with GFP-Merlin isoform 1 from interphasic extracts (I) but much less from mitotic extracts (M). (**B**) Coprecipitation from interphasic Hela cell extracts show that S518D substitution prevent α-tubulin interaction. In contrast, T581D substitution promotes the interaction. Double AA and DD mutants coprecipitation experiments show that S518 substitution is dominant over T581. (**C**) Merlin isoform 2 (Iso2) interacts more strongly with α-tubulin than isoform 1 (Iso1) in Hela interphasic extracts. (**D**) As observed for Merlin isoform 1, GFP-Merlin isoform 2 binding to α-tubulin strongly decrease during mitosis but the overall binding is higher than for Isoform 1. (**E**) S518D substitution inhibits Merlin isoform 2 interaction with α-tubulin assessed by coimmunoprecipitation from Hela interphasic extracts. Average relative α-tubulin binding from at least 3 experiments is indicated. (**F**) S518D substitution stimulates the binding of GFP-C-ter. Merlin (330-595) isoform 1 to purified GST N-ter Merlin (1-330). T581D substitution inhibits the interaction compared to T581A substitution. AA and DD C-terminal Merlin show minimal difference in binding to N-ter Merlin (left panel). Remarkably, the alanine mutation of T581 greatly facilitates the binding of the C-terminal half of Merlin fused to GFP to the his-tagged FERM domain of Ezrin, when compared to the T581D substitution. The binding is even stronger when S518 is also mutated to an alanine (AA) (right panel). The blot shows the quantity of bait protein used (GFP constructs) and the amount of interacting Merlin or Ezrin N-ter protein precipitated. All experiments were repeated at least 3 independent times. Student t-test. ns: $p>0.05$, *: $p<0.05$, **: $p<0.01$, ***: $p<0.001$. Error bars represent ±S.D. GFP was used as a control.

Figure 5

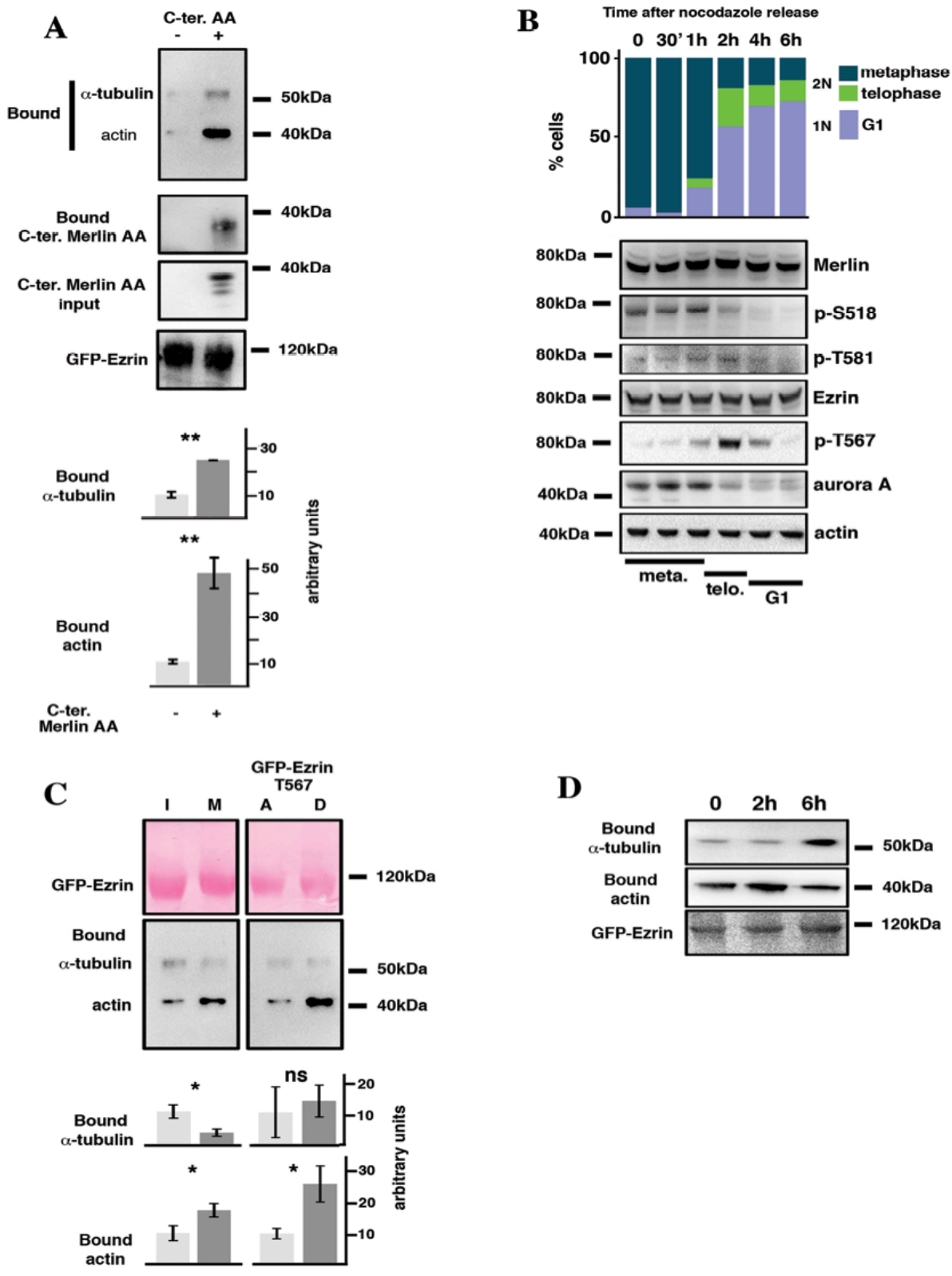

Figure 5: Merlin and Threonine 567 phosphorylation modulate Ezrin interaction with the cytoskeleton during mitosis. (**A**) Merlin C-ter AA domain binds to Ezrin and stimulates its interaction with α-tubulin and actin. Merlin C-ter AA domain was co-expressed (+) or not (-) with GFP-Ezrin in Hela cells. Bound α-tubulin and actin were evaluated by western-blot following precipitation of GFP-Ezrin. (**B**) The expression and phosphorylation of Merlin (S518 and T581), Ezrin (T567) and Aurora A were evaluated by western-blot following the release of Hela cells from nocodazole block. Actin was used as loading control. The progression from mitosis (metaphase and telophase, 2N cells) to G1 (1N cells) was followed by FACS and by microscopy using DAPI staining (upper bar graph). The timeframe showing the progression of the cells through metaphase and telophase, assessed by DAPI staining, is shown under the blots. (**C**) Immunoprecipitation of GFP-Ezrin shows that its binding to α-tubulin decreases whereas interaction with actin increases during mitosis compared to interphase. In addition, T567D substitution stimulates actin binding of Ezrin but has no impact on α-tubulin interaction, when compared to T567A substitution. A quantification of 3 independent experiments is provided. Student t-test: ns: $p>0.05$, *: $p<0.05$, **: $p<0.01$, ***: $p<0.001$. (**D**) The binding of actin and α-tubulin to GFP-Ezrin was followed by coimmunoprecipitation during the transition from mitosis to G1 following release from nocodazole block in Hela cells.

Figure 6

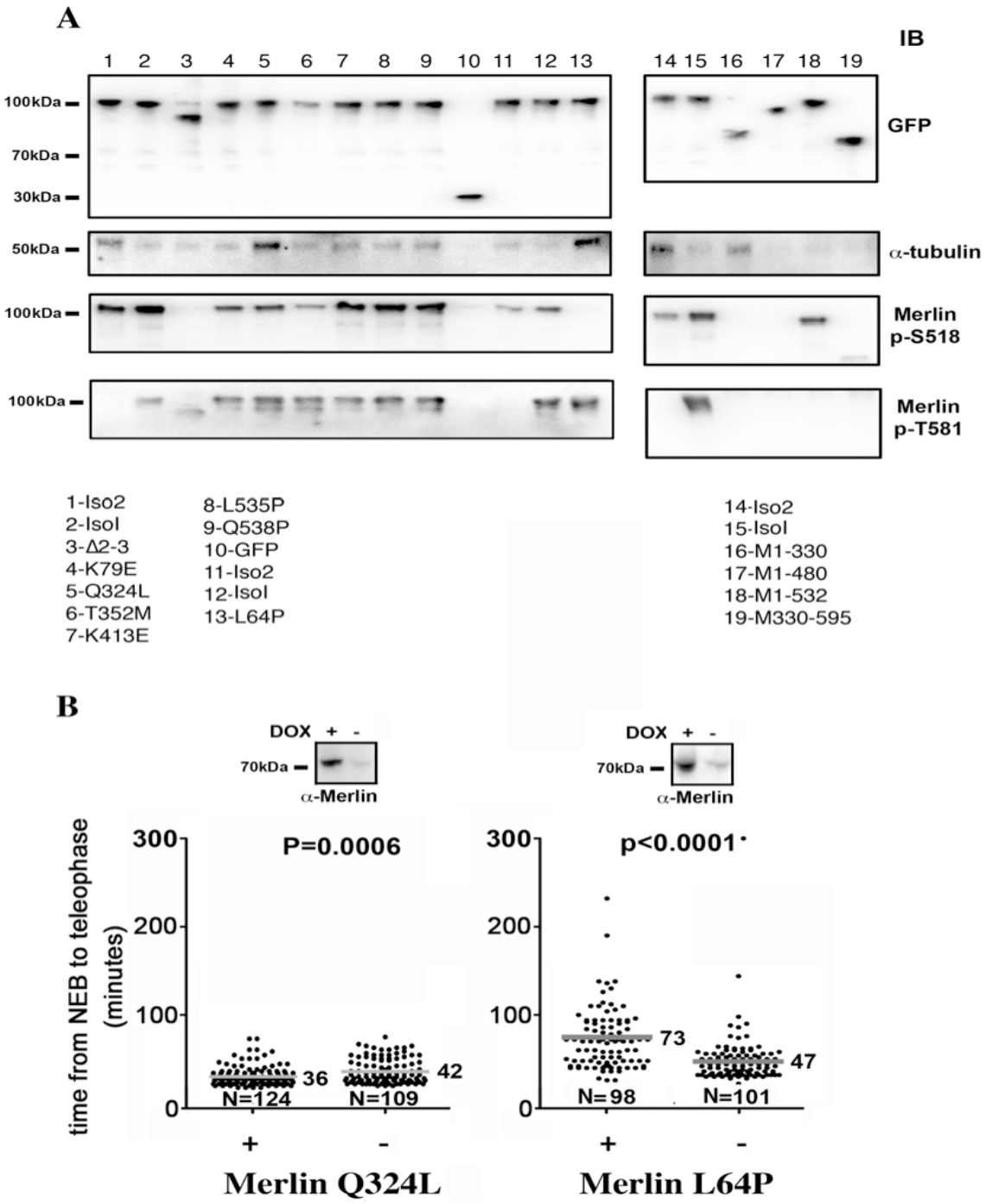

Figure 6: Several patient mutations affect Merlin phosphorylation state and/or the binding to α-tubulin. **(A)** The binding of α-tubulin and the phosphorylation state of S518 and T581 of Merlin isoform 1 and 2, truncation mutants as well as several patient missense mutants were evaluated using HEK293 cells transfected with GFP-Merlin constructs. The expression level of the constructs is presented in the upper panel (probed with anti-GFP antibody). The list of constructs used is indicated below the western-blots. GFP was used as IP control throughout. **(B)** Merlin Q324L expression in Hela cells leads to a limited shortening of mitosis duration. In contrats, L64P mutant strongly delays NEB to telophase progression in a way very similar to Merlin S518A-T581A mutant (Figure 3A&B). Mann Whitney test on R Software.

Figure 7

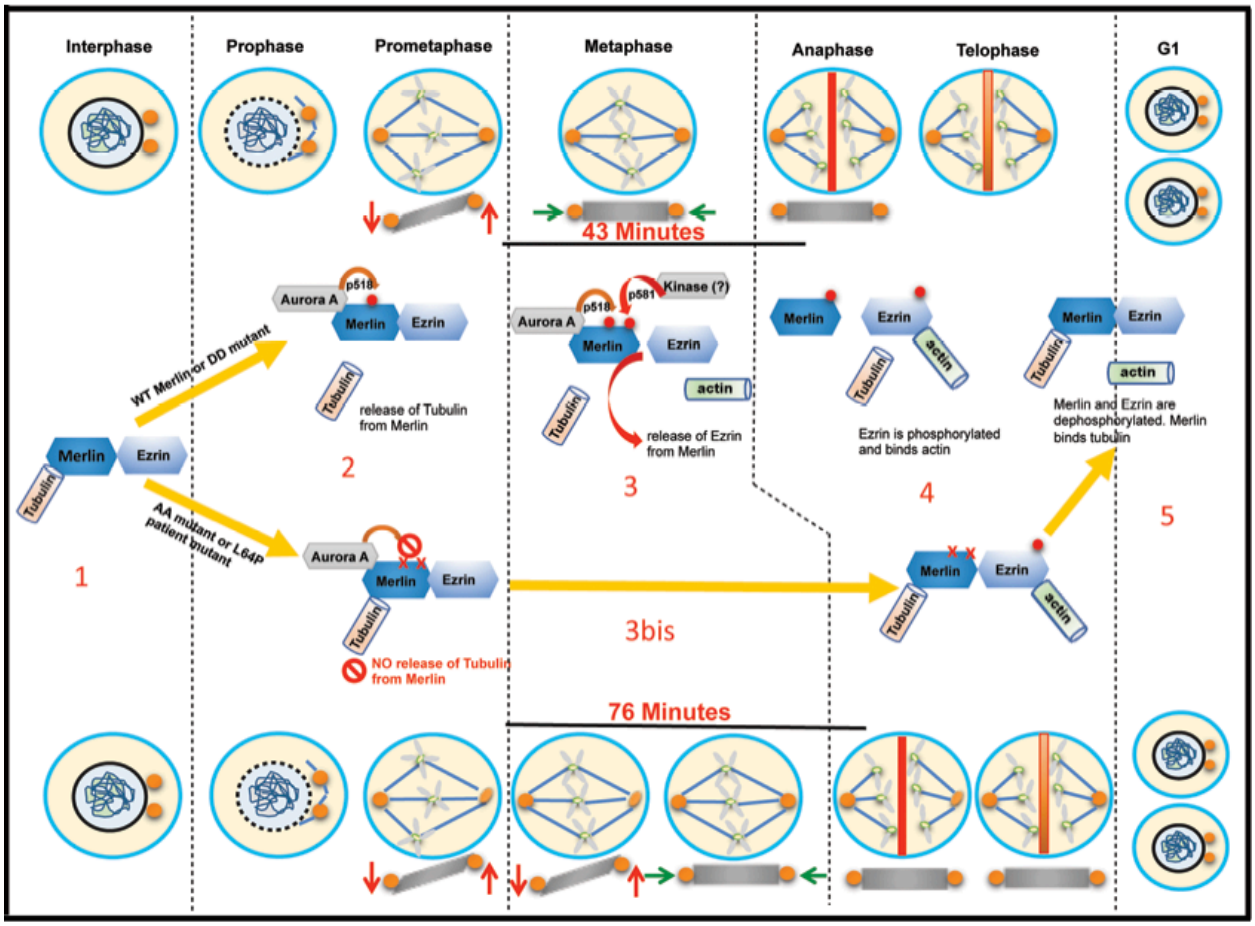

Figure 7: Schematic of Merlin phosphorylation events and interactions with Tubulin and Ezrin during mitosis. During interphase (1) wild-type merlin phosphorylation levels on S518 and T581 are low allowing binding to Tubulin and Ezrin. Upon progression to metaphase (2), S518 is phosphorylated (●) by Aurora-A facilitating phosphorylation of T581. This dual phosphorylation (●●) peaks in metaphase and weakens Merlin interaction with Tubulin and Ezrin (3). Centrosomes position stabilizes in the same plane ( ) , followed by sister chromatids separation ( ) during anaphase. Non-phosphorylable Merlin AA mutant, as well as L64P retain a strong binding to Tubulin and Ezrin correlating with a delay in stabilization ( ) of the centrosome position and progression to anaphase (3bis). Upon progression toward telophase, Ezrin get phosphoryalted on T567 allowing binding to Actin whereas Merlin is progressively dephosphoryated (4). In G1, phosphorylation of Merlin and Ezrin are back to interphasic levels again (5).

Phosphorylation of Merlin by Aurora A kinase appears necessary for mitotic progression

Vinay Mandati, Laurence Del Maestro, Florent Dingli, Bérangère Lombard, Damarys Loew, Nicolas Molinie, Stephane Romero, Daniel Bouvard, Daniel Louvard, Alexis M. Gautreau, Eric Pasmant and Dominique Lallemand

J. Biol. Chem. published online July 11, 2019
